Cellular/Molecular

Altered Neuronal Excitability in Cerebellar Granule Cells of Mice Lacking Calretinin

David Gall,[1] Céline Roussel,[1] Isabella Susa,[2] Egidio D'Angelo,[3,4] Paola Rossi,[3] Bertrand Bearzatto,[1] Marie Christine Galas,[1] David Blum,[1] Stéphane Schurmans,[5] and Serge N. Schiffmann[1]

[1]Laboratoire de Neurophysiologie (CP601), Faculté de Médecine, Université Libre de Bruxelles, B-1070 Bruxelles, Belgium, [2]Optique Nonlinéaire Théorique (CP231), Faculté des Sciences, Université Libre de Bruxelles, B-1050 Bruxelles, Belgium, [3]Department of Cellular and Molecular Physiology and Pharmacology, University of Pavia and Instituto Nazionale per la Fisica della Materia, I-27100 Pavia, Italy, [4]Department of Evolutionary and Functional Biology, University of Parma, 43100 Parma, Italy, and [5]Institut de Biologie et de Médicine Moléculaires (CP300), Université Libre de Bruxelles, B-6041 Gosselies, Belgium

Calcium-binding proteins such as calretinin are abundantly expressed in distinctive patterns in the CNS, but their physiological function remains poorly understood. Calretinin is expressed in cerebellar granule cells, which provide the major excitatory input to Purkinje cells through parallel fibers. Calretinin-deficient mice exhibit dramatic alterations in motor coordination and Purkinje cell firing recorded *in vivo* through unknown mechanisms. In the present study, we used patch-clamp recording techniques in acute slice preparation to investigate the effect of a null mutation of the calretinin gene on the intrinsic electroresponsiveness of cerebellar granule cells at a mature developmental stage. Calretinin-deficient granule cells exhibit faster action potentials and generate repetitive spike discharge showing an enhanced frequency increase with injected currents. These alterations disappear when 0.15 mM of the exogenous fast-calcium buffer BAPTA is infused in the cytosol to restore the calcium-buffering capacity. A proposed mathematical model demonstrates that the observed alterations of granule cell excitability can be explained by a decreased cytosolic calcium-buffering capacity resulting from the absence of calretinin. This result suggests that calcium-binding proteins modulate intrinsic neuronal excitability and may therefore play a role in information processing in the CNS.

Key words: **calretinin; calcium-binding protein; cerebellar granule cell; excitability; calcium; mathematical model**

Introduction

Calcium regulates a large variety of neuronal functions, including neurotransmitter release, ionic channel permeability, enzyme activity, and gene transcription. Hence, the cytosolic calcium concentration must be tightly regulated. Cytoplasmic calcium-binding proteins play a key role in this regulation leading to specific adjustments of neuronal signaling. Among these, calretinin is the only calcium-binding protein known to be expressed in cerebellar granule cells (Résibois and Rogers, 1992; Marini et al., 1997), whereas the structurally related calbindin is exclusively expressed in Purkinje cells. Granule cells form the largest neuronal population in the mammalian brain. They process information entering into the cerebellar cortex through the mossy fibers (Ito, 1984) and convey the major excitatory afference to Purkinje cells through the parallel fibers. The involvement of the cerebellum in motor coordination has long been recognized and, interestingly, it has been shown recently that calretinin-deficient mice ($Cr^{-/-}$) were impaired in motor coordination tests and displayed alterations in Purkinje cell activity recorded *in vivo* (Schiffmann et al., 1999). Because calretinin is not expressed in Purkinje cells, the latter study lacked direct evidence for intrinsic cerebellar electrophysiological alteration at the cellular level, resulting from the $Cr^{-/-}$ mutation. This is particularly relevant, because granule cells show a calcium-dependent regulation on their intrinsic excitability (D'Angelo et al., 1997, 1998, 2001; Gabbiani et al., 1994), so that alteration in calcium buffering is expected to affect action potential generation. Thus, in addition to addressing a question specific to cerebellar physiology, $Cr^{-/-}$ mice may provide a model for understanding the regulation of calcium-dependent control of neuronal excitability.

In this study, we directly address this question by recording granule cells using the perforated patch configuration of the patch-clamp technique in brain slices. We show that the electroresponsiveness of granule cells from $Cr^{-/-}$ mice is altered. Furthermore, we show that intrinsic excitability of granule cells from $Cr^{-/-}$ mice can be restored to its control level by the infusion of an exogenous calcium buffer in the cytosol by means of the whole-cell configuration. Finally, we present a mathematical model providing a link between the observed alterations in gran-

Received Feb. 5, 2003; revised May 16, 2003; accepted Aug. 15, 2003.

This work was supported by the Belgian Fonds pour la Recherche dans l'Industrie et l'Agriculture (C.R., B.B.), Queen Elisabeth Medical Foundation (Neurobiology 99-01 and 02-04), Fund for Medical Scientific Research (Belgium 3.4551.98/3.4507.02), Fondation David et Alice Van Buren, Action de Recherche Concertée (2002-2005), and the European Commission's Fifth Framework Program for Research (Cerebellum BIO4CT98-0182 and Spikeforce IST35271). We thank Philippe Lebrun and Geneviève Dupont for helpful comments. We also thank Albert Goldbeter for providing computing facilities. D.G. is a postdoctoral researcher at the Belgian Fonds National de la Recherche Scientifique (FNRS). M.C.G. is a researcher at the French Centre National de la Recherche Scientifique and a postdoctoral fellow at the Belgian FNRS, and D.B. is a postdoctoral fellow at the Belgian FNRS.

Correspondence should be addressed to Dr. Serge Schiffmann, Laboratoire de Neurophysiologie (CP601), Université Libre de Bruxelles, Route de Lennik 808, B-1070 Bruxelles, Belgium. E-mail: sschiffm@ulb.ac.be.

 0270-6474/03/239320-08$15.00/0

ule cell electroresponsiveness and the decreased cytosolic Ca^{2+}-buffering capacity, resulting from the absence of calretinin. Our results suggest a critical role for calretinin in regulating granule cell excitability and signal coding at the input stage of the cerebellum.

Materials and Methods

Mice. Sex- and age-matched wild-type (WT) and $Cr^{-/-}$ mice backcrossed on a C57BL/6 genetic background (f7) were used in all experiments (Schurmans et al., 1997).

Electrophoresis and immunoblotting. One dimensional polyacrylamide gel electrophoresis was performed as described previously (Galas et al., 2000). Cerebellum from WT and $Cr^{-/-}$ were homogenized in lysis buffer (10 μl/mg of tissue) (M-PER; Pierce, Rockfold, IL) containing a protease inhibitor mixture (Complete; Roche Molecular Biochemicals, Vilvorde, Belgium). Samples were stored at −20°C until analysis. Protein concentrations were determined using MicroBCA Protein Assay (Pierce). Equal amounts of protein (40 μg or 250 μg for the densitometrical analysis) were denatured in 2× Laemmli buffer at 100°C for 5 min and then separated on an SDS-PAGE. Proteins were transferred to supported nitrocellulose (Bio-Rad, Hercules, CA) at 250 mA for 90 min at 4°C. The membrane was blocked with 5% BSA and 0.1% Tween 20 in PBS buffer. The membrane was then incubated with the primary antibody anti-calretinin (1:10000; Swant, Bellinzona, Switzerland) or the primary antibody anti-actin (1:2000; Sigma, St. Louis, MO) overnight at 4°C. After washing in 0.1% Tween 20 containing PBS buffer, the membrane was incubated with the HRP-labeled secondary antibody (anti-rabbit IgG; NEN, Boston, MA) at a concentration of 0.1 μg/ml for 60 min at room temperature. Immunoreactive bands were visualized by chemiluminescent ECL Plus western blotting reagents (Amersham Biosciences, Buckinghamshire, UK). For the densitometrical analysis, the bands on the ECL hyperfilm (Amersham Biosciences) corresponding to calretinin and actin were scanned and quantified using the public domain NIH Image β 4.0.2 program (National Institutes of Health, Bethesda, MD). The ratio between calretinin and actin in the cerebellum is considered 100%.

Immunocytochemistry. Mice were killed by decapitation after a slight ether anesthesia, and brains were removed and fixed in 0.1 M phosphate-buffered 4% paraformaldehyde freshly prepared for 24 hr at 4°C. Brains were then rinsed in several changes of 0.1 M PBS, pH 7.4, and cryoprotected in sucrose. Cryostat-cut 30 μm thick brain coronal sections were processed free-floating. After quenching of the endogenous peroxydases, the floating sections were incubated for 1 hr in 10% swine normal serum (Hormonologie Laboratoire, Marloie, Belgium). Sections were then incubated overnight at room temperature with anti-calretinin polyclonal antiserum (1/1000; Swant). Thereafter, they were successively incubated with swine anti-rabbit gammaglobulins (1/30; Dako, Glostrup, Denmark) and rabbit PAP complex (1/300; Dako). The peroxydase activity was revealed by diaminobenzidine in the presence of hydrogen peroxide.

Histology. Four wild-type and four calretinin-deficient mice were killed, and their brains were removed and fixed overnight in 4% paraformaldehyde. After a wash in 0.1 M PBS and consecutive 24 hr incubations in 10, 20, and 30% sucrose solutions, brains were frozen in isopentane. Sagittal sections (15 μm) were performed at the level of the vermis using a cryotome (Leica, Wetzlar, Germany) and stained using a Nissl procedure. For each mouse, four digitized fields (100 × 100 μm) were randomly generated from four adjacent stained sections at a 63× magnification using a confocal microscope (Bio-Rad). On each field, we measured the surface of 10 individual granule cells using the Scion–NIH Image software. The mean apparent area of granule cells was then determined for each mouse, and the difference between genotypes was compared using unpaired Student's *t* test.

Whole-cell patch-clamp recordings. Cerebellar granule cells were recorded in acute cerebellar slices obtained from 15- to 31-d-old mice, when the excitable response has assumed its mature pattern (D'Angelo et al., 1997). Slice preparations were performed as described previously (D'Angelo et al., 1998). Current-clamp recordings were taken from granule cells in the internal granular layer at room temperature using the "blind patch" approach. All recordings were made with an EPC-8 amplifier (Heka Elektronik, Lambrecht/Pfalz, Germany) in the fast current-clamp mode. Membrane potential signal was filtered using an 8-pole Bessel low-pass filter (Frequency Devices, Haverhill, MA) at a cutoff frequency of 2 KHz and subsequently digitized at 10 kHz using the acquisition software Pulse (Heka) in combination with an ITC-16 analog-to-digital converter (InstruTech, Port Washington, NY). Patch pipettes were pulled from borosilicate glass capillaries (Harvard Apparatus, Edenbridge, UK) and had a resistance of ~6 MΩ. For whole-cell recordings, the pipette solution contained the following (in mM): 126 KGluconate, 0.05 $CaCl_2$, 0.15 BAPTA, 4 NaCl, 1 $MgSO_4$, 15 glucose, 5 HEPES, 3 MgATP, and 0.1 GTP, pH adjusted at 7.2 with KOH. Recordings were started 5 min after obtaining the whole-cell configuration to allow diffusion of the calcium buffer BAPTA into the cytosol. In some experiments, the perforated patch configuration of the patch-clamp technique (Horn and Marty, 1988) was used to maintain the endogenous Ca^{2+} buffers. The pipette solution contained the following (in mM): 80 K_2SO_4, 10 NaCl, 15 glucose, and 5 HEPES, pH adjusted at 7.2 with KOH, and 100 μg/ml nystatin. The extracellular solution contained the following (in mM): 120 NaCl, 2 KCl, 2 $CaCl_2$, 1.19 $MgSO_4$, 26 $NaHCO_3$, 1.18 KH_2PO_4, and 11 glucose equilibrated with 95% O_2/5% CO_2, pH 7.4. Intrinsic excitability was investigated by setting resting membrane potential at −80 mV and injecting 1 sec steps of depolarizing current (from 2–30 pA in a 2 pA increment). Action potential frequency was measured by dividing the number of interspike intervals by the time interval between the first and the last spike. The amplitude of the action potential undershoot was estimated as the difference between the threshold of spike prepotential and the minimal potential during spike afterhyperpolarization. When EPSPs were measured, the extracellular solution was supplemented with 25 μM picrotoxin to block GABAergic inhibition generated by Golgi cell synapses (Armano et al., 2000). The mossy fibers were stimulated at a frequency of 0.1 Hz with a bipolar tungsten electrode via a stimulus isolation unit. In our EPSP-recording protocol, 200 μs step current pulses were applied to activate the mossy fibers while measuring EPSPs from a resting potential of −70 mV. The maximal effective stimulus intensity was used in all EPSP recordings. The time to peak was estimated as the interval between the beginning of the stimulating pulse and the maximum of the spike upstroke during the EPSP. The time constant of EPSP relaxation, τ_{decay}, was estimated by monoexponential fitting using the Levenberg–Marquardt algorithm implemented in IGOR (WaveMetrics, Lake Oswego, OR). Only EPSPs giving rise to action potentials were used to evaluate the number of spikes per EPSP. Passive cellular parameters were extracted in voltage clamp by analyzing current relaxation induced by a 10 mV step change from a holding potential of −70 mV as described previously (D'Angelo et al., 1995). In the perforated patch configuration, access resistance was monitored to ensure that voltage attenuation in current-clamp mode was always <10%. Data are reported as means ± SEM, and statistical comparisons were performed using unpaired Student's *t* test [$p > 0.05$, not significant (NS)].

Minimal model of the granule cell. Calcium dynamics have a profound influence on Ca^{2+}-activated K^+ current ($I_{K\text{-}Ca}$) activation, thereby regulating spike discharge. A typical approach to investigate Ca^{2+} dynamics (Traub and Llinas, 1979) is to model Ca^{2+} and $I_{K\text{-}Ca}$ and to adapt Ca^{2+} dilution and removal to match the firing pattern. This approach has been applied previously to cerebellar granule cell model (Gabbiani et al., 1994; Maex and Schutter, 1998; D'Angelo et al., 2001). Here, to focus our attention on Ca^{2+} dynamics, we reduced the number of gating variables and currents involved in action potential generation. We also modified the equation governing the Ca^{2+} dynamics to take into account variations in the concentration of endogenous Ca^{2+} buffers.

Because granule cells have a compact electrotonic structure (Silver et al., 1992; D'Angelo et al., 1993, 1995, 2001), a single compartment model was used. Following the classical Hodgkin and Huxley (1952) approach, the membrane can be considered as a leaky capacitor, and the membrane potential dynamics are governed by the following current balance equation:

$$C_m \frac{dV}{dt} = -I_{Na} - I_{K-V} - I_{Ca} - I_{K-Ca}, \quad (1)$$

where C_m is cell capacitance, I_{Na} is a voltage-dependent Na^+ current, $I_{K\text{-}V}$ is a delayed rectifier K^+ current, I_{Ca} is a high-threshold voltage-

Table 1. Voltage-dependent conductance parameters

Conductance state, variable	n	G_{max} (nS)	V_{rev} (mV)	α (msec^{-1})	β (msec^{-1})	τ_{min} (msec)
g_{Na}						
Activation, m	3			7.5 exp [0.081(V + 39)]	7.5 exp [−0.066(V + 39)]	
Inactivation, h	1	172	55	0.6 exp [−0.089(V + 50)]	0.6 exp [0.089(V + 50)]	0.045
g_{K-v}						
Activation, n	4	28	−90	0.85 exp [0.073(V + 38)]	0.85 exp [−0.018(V + 38)]	
g_{Ca}						
Activation, s	2	58	80	8/(1+exp [−0.072(V−5)])	0.1(V+8.9)/(exp [0.2(V+8.9)]−1)	
g_{K-Ca}						
Activation, a	1	56.5	−90	12.5/(1+[0.15 exp(−0.085V)]/[Ca])	7.5/(1+[Ca]/[0.015 exp(−0.077V)])	

dependent Ca^{2+} current, and $I_{K\text{-}Ca}$ is a Ca^{2+}-activated K^+ current. These ionic currents have been shown to be the core of action potential generation in cerebellar granule cells (D'Angelo et al., 1998) when the excitable response has assumed its mature pattern (D'Angelo et al., 1997). The interplay between I_{Na} and $I_{K\text{-}V}$ is the basic mechanism, giving rise to the action potentials, and the presence of I_{Ca} and $I_{K\text{-}Ca}$ allows coupling between intracellular calcium dynamics and membrane potential dynamics. We also reduced the number of gating variables by exploiting the difference in their time scale compared with the time scale of the evolution of V. The complete expressions for the different ionic currents are given by the following:

$$I_{Na} = \bar{g}_{Na} m_\infty^3 h (V - V_{Na}), \quad (2)$$

$$I_{K-V} = \bar{g}_K n_\infty^4 (V - V_K), \quad (3)$$

$$I_{Ca} = \bar{g}_{Ca} s^2 (V - V_{Ca}), \quad (4)$$

$$I_{K-Ca} = \bar{g}_{K-Ca} a (V - V_K), \quad (5)$$

where the evolution of the gating variables h, s, and a is governed by the following relationships:

$$\frac{dh}{dt} = \frac{h_\infty(V) - h}{\tau_h(V)}, \quad (6)$$

$$\frac{ds}{dt} = \frac{s_\infty(V) - s}{\tau_s(V)}, \quad (7)$$

$$\frac{da}{dt} = \frac{a_\infty(V,\mathrm{Ca}) - a}{\tau_a(V,\mathrm{Ca})}. \quad (8)$$

For a given gating variable, x, the steady state function, x_∞, and the relaxation time constant, τ_x, are related to the corresponding first-order rate functions, α_x and β_x, by the following relationships:

$$x_\infty = \frac{\alpha_x}{\alpha_x + \beta_x}, \tau_x = \frac{1}{\alpha_x + \beta_x}, x = m,h,n,s,a. \quad (9)$$

Channel parameter values are given in Table 1. The gating parameters for I_{Na}, $I_{K\text{-}V}$, I_{Ca}, and the cell capacitance, (C_m = 3.14 pF) are the same as those in Maex and Schutter (1998). The conductances of the different currents and the parameters related to the calcium dependence of $I_{K\text{-}Ca}$ were adapted to obtain current intensities during the action potential similar to those in the models of Gabbiani et al. (1994) and D'Angelo et al. (2001).

To complete the model, the following balance equation gives the evolution of the free calcium concentration (in μM) in a submembrane shell of thickness d in a cell of surface area A.

$$\frac{d\mathrm{Ca}}{dt} = f\left[-\frac{I_{Ca}}{2FAd} - \beta_{Ca}\mathrm{Ca} \right], \quad (10)$$

where the dimensionless parameter f represents the calcium-buffering capacity of the cytosol inside the submembrane shell, resulting from the presence of fast calcium-binding proteins (binding is assumed to be instantaneous). In particular, calretinin is a fast-calcium buffer, the mean free lifetime for a Ca^{2+} ion in the presence of a physiological concentration of the protein of the μs order (Edmonds et al., 2000), third order of magnitude faster than the time scale of the evolution of the system variables. Therefore, any alteration in the calretinin level corresponds to a modification of f. Moreover, because this parameter can be seen as the ratio of free Ca^{2+} concentration to bound Ca^{2+} concentration (Chay and Keizer, 1983; Gall and Susa, 1999; Gall et al., 1999), a decrease in cytosolic Ca^{2+}-buffering capacity, attributable to the absence of calretinin, can be mimicked by an increase in the value of f. In the absence of data for cerebellar granule cells, the numerical values for the cytosolic Ca^{2+}-buffering capacity (in the order of 0.01) have been set in agreement with values reported for other neuronal types (Tatsumi and Katayama, 1993; Stuenkel, 1994; Helmchen et al., 1996), with the notable exception of cerebellar Purkinje cells, which show a calcium-binding ratio of an order of magnitude higher (Fierro and Llano, 1996). The parameter β_{Ca} describes Ca^{2+} removal corresponding to diffusion, action of ionic pumps, and slow buffers. Calcium dynamics were adapted to yield Ca^{2+} transients in the μM range, similar to those reported from Gabbiani et al. (1994). Parameter values are A = 314 (μm)^2, d = 0.084 μm, β_{Ca} = 10 msec^{-1}, and F is the Faraday constant.

Equations 1, 6, 7, 8, and 10 constitute our minimal model for the cerebellar granule cell. The equations of the model are numerically solved using a fourth-order Runge-Kutta method, as implemented in the subroutine D02BBF of the Numerical Algorithms Group library. Computations are performed on an SGI R12000 workstation (Silicon Graphics, Mountain View, CA). To test the accuracy of our minimal model, simulations were also run with similar results (data not shown), with models by Maex and Schutter (1998) and D'Angelo et al. (2001) modified to include Ca^{2+} dynamics as described in Equation 10.

Results

Enrichment of calretinin in the mouse cerebellum

Calcium-binding proteins are differentially expressed depending on the neuronal type. Figure 1*A* shows that calretinin is particularly enriched in the mice cerebellum as compared with other brain areas such as the hippocampus (Schurmans et al., 1997). In this study, the role of calretinin was investigated by using calretinin-deficient mice. Calretinin was revealed by Western blotting with anti-calretinin antiserum. No calretinin signal could be detected in the cerebellum of $Cr^{-/-}$ mice as expected for a null mutation (Fig. 1*B*). In addition, immunocytochemistry revealed no calretinin immunoreactivity in the cerebellar granule cell layer of $Cr^{-/-}$ mice (Fig. 1*C*).

Alteration of granule cell intrinsic membrane excitability

Unless otherwise stated, recordings were made using the perforated patch technique to minimize unwanted alteration of the endogenous Ca^{2+}-buffering capacity. No difference in membrane resistance or capacitance could be observed in $Cr^{-/-}$ compared with wild-type granule cells (Table 2), indicating the absence of granule cell morphological alterations. This was confirmed by the quantitative data we obtained using histological

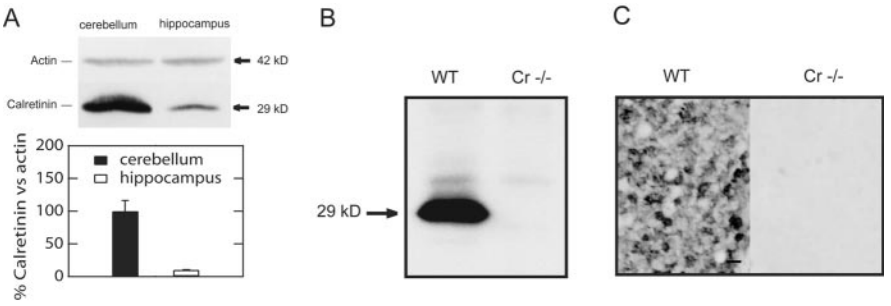

Figure 1. Expression of calretinin in the cerebellum of wild-type mice and absence of calretinin in the cerebellum of mutant mice. The Western blot analysis shown in *A* illustrates the relative distribution of calretinin in the cerebellum and hippocampus of the wild-type mice ($n = 4$). Also shown is a Western blot analysis of cerebellar protein homogenates (*B*) and calretinin-immunoreactivity detection in the granule cell layer (*C*) from $Cr^{-/-}$ mice compared with wild-type mice. Scale bar, 10 μm. No calretinin signal is detected in the $Cr^{-/-}$ mice.

Table 2. Passive membrane properties

	n	V_{rest} (mV)	C_m (pF)	R_{in} (GΩ)
WT	5	−64.8 ± 5.5	2.0 ± 0.2	2.3 ± 0.3
$Cr^{-/-}$	8	−65.9 ± 5.3	2.2 ± 0.4	2.1 ± 0.2

staining and confocal microscopy showing that the mean granule cell-apparent area was similar in both WT (21.8 ± 1.05 μm^2; $n = 4$) and calretinin-deficient mice (20.69 ± 1.28 μm^2; $n = 4$; NS). Moreover, no difference in subthreshold currents measured at −70 and −80 mV could be detected in $Cr^{-/-}$ mice (−1.9 ± 2.0 pA and −7.8 ± 2.0 pA, respectively; $n = 8$) as compared with wild-type granule cells (−2.2 ± 5.7 pA and −7.9 ± 4.8 pA, respectively; $n = 5$; NS).

Intrinsic granule cell electroresponsiveness was investigated in current-clamp recordings. The resting potential of WT and $Cr^{-/-}$ granule cells was not significantly different (−64.8 ± 5.5 mV, $n = 5$ vs −65.9 ± 5.3 mV, $n = 8$; NS). Neither WT nor $Cr^{-/-}$ granule cells generated spontaneous action potentials. Active cell membrane properties were evaluated by measuring the voltage response while injecting steps of depolarizing current of increasing intensities in the granule cell soma. Above a critical value of the injected current (4.4 ± 1.6 pA for WT, $n = 5$ vs 4.9 ± 1.0 pA for $Cr^{-/-}$, $n = 8$; NS), fast repetitive spiking was obtained with a threshold of spike prepotential of −58.0 ± 2.3 mV for WT granule cells ($n = 5$) and −58.7 ± 2.0 mV for $Cr^{-/-}$ granule cells ($n = 8$; NS). Action potentials occurred in regular trains showing little or no adaptation (Fig. 2*A*), and frequency increased with the intensity of the injected current. The average frequency was measured over the entire duration of current injection (1 sec) and was used to construct current–frequency plots (Fig. 2*B*). At low current intensities, the current–frequency plots were interpolated with a straight line. Because the threshold current and maximal frequency varied substantially from cell to cell, the evaluation of the slope factor of the linear part of current–frequency plots was used as a normalized measure of excitability. Using such analysis, we observed a significant increase in the slope of the current–frequency plots (4.8 ± 0.2 Hz·pA^{-1} for WT, $n = 5$ and 6.6 ± 0.7 Hz·pA^{-1} for $Cr^{-/-}$, $n = 8$; $p < 0.05$), indicating that the excitability of $Cr^{-/-}$ granule cells was increased (Fig. 2*C*). In addition, $Cr^{-/-}$ granule cells showed a 23% decrease in the action potential half-width (Fig. 2*D*) evaluated at the threshold potential in which fast repetitive spiking is obtained (1.02 ± 0.06 msec for WT, $n = 5$ and 0.78 ± 0.06 msec for $Cr^{-/-}$, $n = 8$; $p < 0.05$). Besides changes observed in $Cr^{-/-}$ mice, it should be noted that both the spike shape and frequency of spike discharge in WT mice were similar to those reported previously (D'Angelo et al., 1998). The action potential undershoot amplitude was deeper for $Cr^{-/-}$ than WT granule cells, although this change did not reach statistical significance (−4.0 ± 0.7 mV for WT, $n = 5$ and −6.4 ± 1.7 mV for $Cr^{-/-}$, $n = 7$; $p = 0.2406$; NS). The fact that the latter change fails to be statistically significant probably reflects the higher sensitivity of this parameter toward cell-to-cell variations, compared with more robust temporal parameters such as the slope factor of current–frequency relationship or the action potential half-width.

Restoration of neuronal excitability by an exogenous buffer

The lack of calretinin in $Cr^{-/-}$ mice is likely to alter cytosolic Ca^{2+} buffering in cerebellar granule cells. To test this hypothesis, we measured the ability of an exogenous Ca^{2+} buffer to restore similar levels of excitability in the mutant mice as in the WT mice. Because calretinin and BAPTA have similar Ca^{2+}-binding kinetics (Roberts, 1993; Edmonds et al., 2000), we perfused the cells with 0.15 mM BAPTA using the whole-cell configuration of the patch-clamp technique. In these conditions, no differences between the mutant and the WT mice could be found (Fig. 3) either concerning spike-discharge frequency (4.4 ± 0.3 Hz·pA^{-1} for WT, $n = 5$ and 4.4 ± 0.4 Hz·pA^{-1} for $Cr^{-/-}$, $n = 5$) or action potential half-width (0.59 ± 0.07 msec for WT, $n = 50$ and 0.64 ± 0.06 msec for $Cr^{-/-}$, $n = 5$). The difference in action potential half-width observed in WT granule cells using the whole-cell configuration, compared with the corresponding value measured using the perforated patch method, is probably a consequence of the difference between the two recording conditions. Indeed, the higher series resistance obtained in perforated patch configuration determines a voltage attenuation (D'Angelo et al., 1995) that could slightly alter the spike shape but not the spike count. Therefore, we can compare the slope factors obtained in the two recording conditions. Our results show that the presence of 0.15 mM BAPTA in the pipette is sufficient to restore an excitability level in the $Cr^{-/-}$ granule cell similar to the one measured in the WT using the perforated patch method. This indicates that the endogenous cytosolic Ca^{2+}-buffering capacity in the cerebellar granule cell is approximately equivalent to 0.15 mM BAPTA.

We also studied the effect of a decreased calcium-buffering capacity on granule cell excitability by performing whole-cell recording with low BAPTA concentration (0.01 mM) on wild-type mice. In these conditions, we observe an important spike-frequency accommodation (data not shown) in all of our recordings ($n = 7$). The absence of a stable repetitive firing pattern prevented us from estimating accurately the average action potential frequency at a given injected current and thus to construct current–frequency plots. Therefore, the intrinsic excitability cannot be evaluated in a similar way as the previous recordings. In addition, the spike-frequency accommodation alters the action potential kinetics, preventing us from accurately measuring the action potential half-width. Such modulation of spike-frequency accommodation by changes in calcium-buffering capacity has been shown to occur in hippocampal neurons (Lancaster and Nicoll, 1987). The absence of a similar increase in spike-frequency accommodation in the perforated patch recording on

the $Cr^{-/-}$ granule cells indicates the existence of compensatory mechanisms at work in the mutant.

Relationship between calretinin deficiency and altered excitability

To investigate the role of cytosolic Ca^{2+} buffering on intrinsic granule cell excitability, we used a mathematical model (see Materials and Methods). This model should be seen as a minimal model allowing us to qualitatively understand the impact of variations in cytosolic Ca^{2+}-buffering capacity on the electroresponsiveness of an excitable cell. Nevertheless, parameter values have been chosen to reproduce the relevant aspects of the cerebellar granule cell electroresponsiveness. Figure 4*A* shows the model response to an intrasomatic injection of a 14 pA depolarizing current. In our model, calcium-buffering capacity, resulting from the action of fast-calcium buffers, is represented by the dimensionless parameter *f* giving the ratio of free Ca^{2+} concentration to bound Ca^{2+} concentration (Chay and Keizer, 1983; Gall and Susa, 1999; Gall et al., 1999). A decrease in cytosolic Ca^{2+}-buffering capacity, resulting from the absence of calretinin, can be simulated by an increase in the value of *f*. The observed alterations in $Cr^{-/-}$ mice can be mimicked by a fourfold decrease in the cytosolic Ca^{2+}-buffering capacity, raising the action potential frequency from 55.1 ($f = 0.01$) to 105.7 Hz ($f = 0.04$) in good agreement with the experimental data (Fig. 2*A*). The linear slope increase in current–frequency plots from 3.0 Hz·pA^{-1} for $f = 0.01$ to 5.2 Hz·pA^{-1} for $f = 0.04$ (Fig. 4*B*) is also close to the experimental values. Figure 5 shows the effect of a fourfold decrease of the cytosolic Ca^{2+}-buffering capacity on membrane voltage, submembrane Ca^{2+} concentration, and membrane currentsduring an action potential. The action potential half-width undergoes a 41% decrease when *f* is increased from 0.01 to 0.04. This action potential shortening reflects a more pronounced activation of $I_{K\text{-}Ca}$ because of faster Ca^{2+} dynamicstaking place when the cytosolic Ca^{2+}-buffering capacity is decreased. This greater $I_{K\text{-}Ca}$ activation also leads to a 28% increase in the action potential undershoot. Therefore, the model suggests that the faster Ca^{2+} dynamics can fully explain the increased excitability observed in $Cr^{-/-}$ mice through increased activation of Ca^{2+}-activated K^+ current. It is important to note that a change in the dynamics leading to the activation of $I_{K\text{-}Ca}$ is needed to obtain hyperexcitability in the model. A simple increase in the maximal conductance, attributable to Ca^{2+}-activated K^+ channels ($\bar{g}_{K\text{-}Ca}$), leads to the opposite effect, lowering the spike frequency (data not shown). Finally, because our model is a qualitative one, we do not claim that the fourfold variation in *f* represents the actual variation of the calcium-buffering capacity resulting from the absence of calretinin. A quantitative analysis would require a detailed knowledge of the mechanisms regulating the Ca^{2+} homeostasis of the cerebellar granule cell. Such a complete set of quantitative data is not available at the present time. Similar results (date not shown) were obtained with models by Maex and Schutter (1998) and D'Angelo et al. (2001), which were modified to include Ca^{2+} dynamics as described by Equation 10.

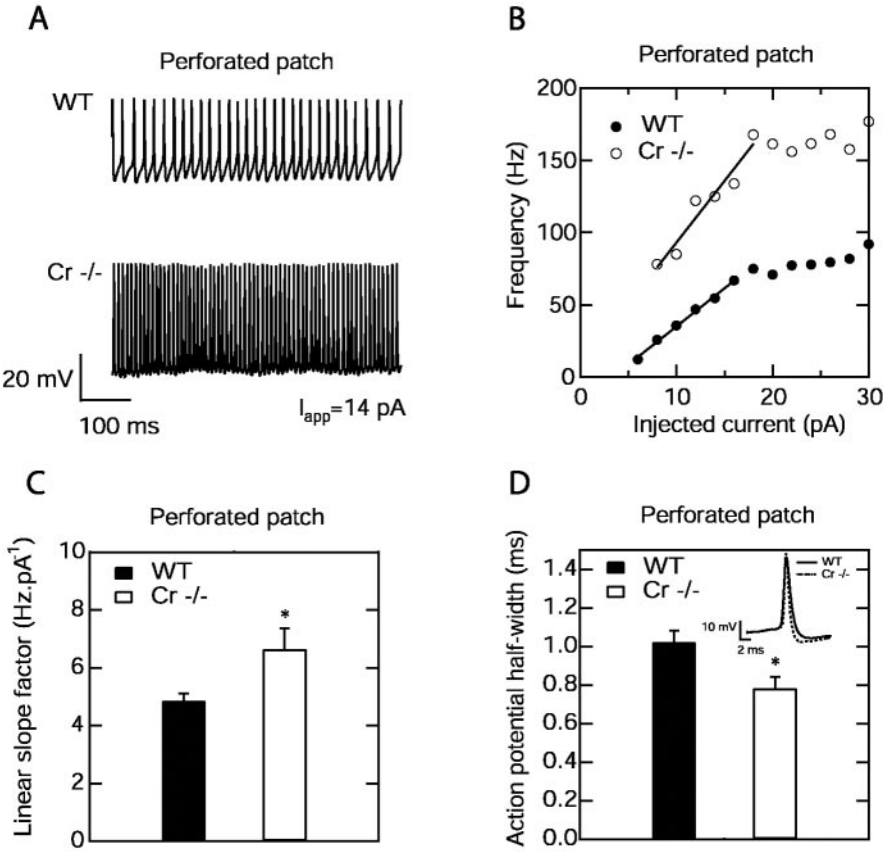

Figure 2. Evaluation of the intrinsic excitability of a cerebellar granule cell in wild-type and $Cr^{-/-}$ mice. *A*, Repetitive spiking obtained by the injection of a 14 pA depolarizing current in a WT granule cell (top) and a $Cr^{-/-}$ granule cell with similar threshold current for action potential generation. The $Cr^{-/-}$ granule cell shows a much higher action potential frequency (*A*, bottom) and faster action potentials (*D*, inset) compared with the WT cell for the same injected current from a holding potential of −80 mV. Because the frequency remained stable throughout the stimulation, average frequency was measured over the total time of current injection (1 sec) at increasing intensities. From this data, current–frequency plots could be constructed (*B*). At low-current intensities, granule cells showed a linear encoding of stimulus intensity. The slope of the linear part of current–frequency plots was used as a measure of the intrinsic granule cell excitability. Histograms report the slope factor of current–frequency plots for WT vs $Cr^{-/-}$ (*C*) and corresponding durations of action potentials at half-amplitude (*D*) evaluated at the threshold potential where fast repetitive spiking is obtained. In the perforated patch configuration, $Cr^{-/-}$ granule cells ($n = 8$) show significantly ($^*p < 0.05$) increased excitability and faster action potentials ($^*p < 0.05$) compared with WT ($n = 5$).

Unaltered synaptic transmission

We have also examined whether the absence of calretinin also affects synaptic transmission at the mossy fiber–granule cell synapse. Granule cells are excited by glutamatergic mossy fiber synapses and inhibited by GABAergic Golgi cell synapses. Without $GABA_A$ receptor inhibitors, mossy fiber stimulation in sagittal cerebellar slices causes strong granule cell inhibition through direct activation of Golgi cells by the mossy fibers (Armano et al., 2000). Therefore, to measure the EPSPs, we stimulated mossy fibers in the presence of the $GABA_A$ receptor-blocker picrotoxin (25 μM). In these conditions, a similar increase in the intrinsic excitability was observed, because the slope of the current–frequency plots was significantly higher in mutant mice (3.4 ± 0.6 Hz·pA^{-1} for WT, $n = 6$ and 7.3 ± 1.0 Hz·pA^{-1} for $Cr^{-/-}$, $n = 5$; $p < 0.05$). However, no differences in the EPSP amplitude or kinetics could be observed (Fig. 6, Table 3).

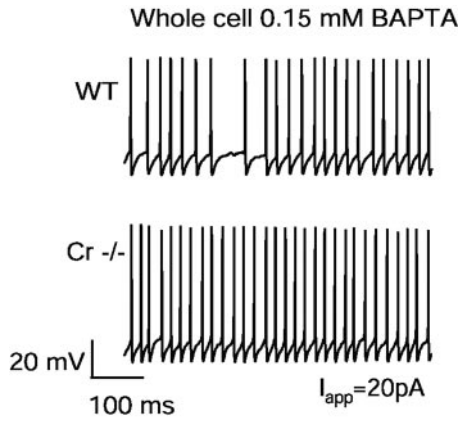

Figure 3. Restauration of neuronal excitability by the exogenous Ca^{2+} buffer BAPTA. In the whole-cell configuration, the presence of 0.15 mM BAPTA in the pipette solution is able to restore a similar excitability level in the WT and $Cr^{-/-}$ mice.

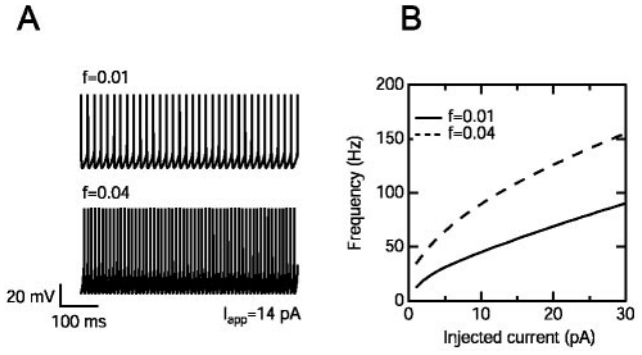

Figure 4. Effect of a reduction of the Ca^{2+}-buffering capacity on the intrinsic excitability of the granule cell model. *A*, The response of the granule cell model to injection of a 14 pA depolarizing current with a cytosolic Ca^{2+}-buffering capacity parameter *f* of 0.01 (top) and 0.04 (bottom) is shown. The increase in parameter *f* mimics the decrease in cytosolic Ca^{2+}-buffering capacity, resulting from the absence of calretinin (see Materials and Methods). *B*, Corresponding current–frequency plots. The curves are obtained by numerical integration of Equations 1, 6, 7, 8, and 10. Parameter values are listed in Materials and Methods. As observed experimentally, action potentials are faster, and the slope of the current–frequency plot is markedly increased.

Discussion

This study shows that the absence of calretinin increases cerebellar granule cell excitability without altering granule cell morphology or passive electrical membrane properties. Calretinin is a Ca^{2+}-binding protein member of the "EF-hand" family (Persechini et al., 1989). On the basis of available functional data, two types of EF-hand Ca^{2+}-binding proteins can be distinguished. Proteins like calmodulin change their conformation after Ca^{2+} binding, thereby modulating the activity of various enzymes (Cheung, 1980) and ionic channels (Peterson et al., 1999; Qin et al., 1999; Zuhlke et al., 1999). In contrast, proteins like parvalbumin, calbindin-D28K, and calretinin are believed to play the role of passive-buffering systems, limiting the rise in intracellular free Ca^{2+} concentration.

We used a mathematical model to examine whether the observed alterations of $Cr^{-/-}$ cerebellar granule cell electroresponsiveness could be linked to the decreased Ca^{2+}-buffering capacity determined by the absence of calretinin. When challenged with a decreased cytosolic Ca^{2+}-buffering capacity, the model correctly predicts all of the changes in $Cr^{-/-}$ granule cell electroresponsiveness that are observed experimentally. Thus, calretinin seems to affect excitability primarily by acting as a passive Ca^{2+} buffer.

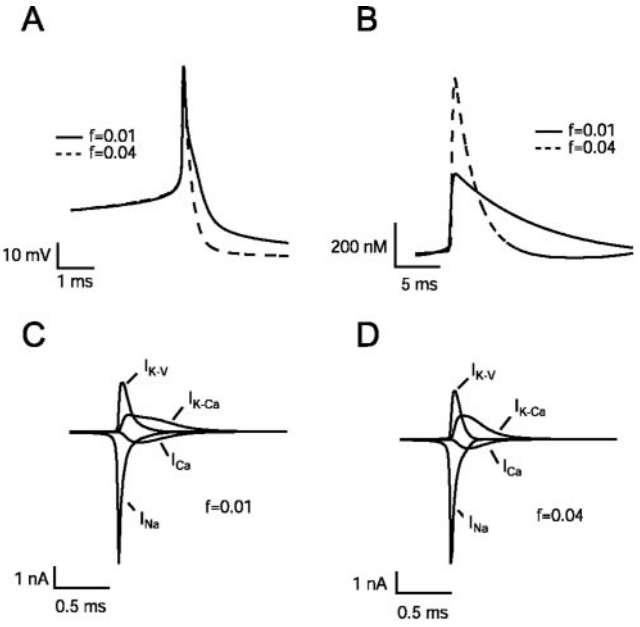

Figure 5. Effect of a reduction of the Ca^{2+}-buffering capacity on the action potential, submembranous Ca^{2+} concentration, and ionic currents of the granule cell model. *A*, *B*, Superposition of the action potentials (*A*) elicited by a 4 pA depolarizing current and corresponding Ca^{2+} transients in the submembrane shell (*B*) with a cytosolic Ca^{2+}-buffering capacity parameter *f* of 0.01 (solid line) and 0.04 (dashed line). *C*, *D*, The corresponding time courses of ionic currents flowing across the membrane during the action potential for $f = 0.01$ (*C*) and $f = 0.04$ (*D*). I_{Na}, Voltage-dependent Na^+ current; $I_{K\text{-}V}$, delayed rectifier K^+ current; I_{Ca}, high-threshold Ca^{2+} current; $I_{K\text{-}Ca}$, Ca^{2+}-activated K^+ current. Action potentials are shorter when the buffering capacity is decreased. The decreased cytosolic Ca^{2+}-buffering capacity allows higher and faster Ca^{2+} transients, leading to a more pronounced activation of $I_{K\text{-}Ca}$, whereas the other currents remain mostly unchanged.

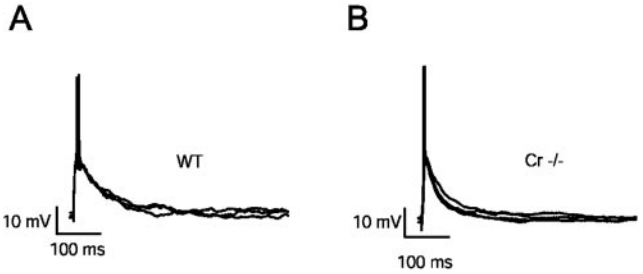

Figure 6. No change in synaptic excitation of $Cr^{-/-}$ cerebellar granule cells. *B*, Superposition of three traces corresponding to the synaptic responses elicited by mossy fiber stimulation from a membrane potential of −70 mV in the presence of 25 μM picrotoxin in a wild-type granule cell (*A*) and $Cr^{-/-}$ granule cell (*B*). The absence of calretinin does not induce alterations in EPSP characteristics (Table 3).

A direct confirmation of this conclusion is provided by the fact that 0.15 mM BAPTA is able to restore normal excitability levels in $Cr^{-/-}$ granule cells. A consequence of this observation is that, because calretinin and BAPTA have similar Ca^{2+}-binding kinetics and because calretinin is the only calcium-binding protein detected so far in cerebellar granule cells, 0.15 mM BAPTA may effectively mimic the contribution of calretinin to the cytosolic Ca^{2+}-buffering capacity of the granule cell. Finally, the similar intrinsic excitability in the wild-type and $Cr^{-/-}$ mice observed in the presence of 0.15 mM BAPTA supports the notion that the membrane properties involved in the action potential generation are similar in the two strains. Thus, the possibility that the increased excitability observed in $Cr^{-/-}$ mice in the perforated

Table 3. EPSP characteristics

	n	Amplitude (mV)	Time to peak (msec)	τ_{decay} (msec)	Spike number
WT	6	17.8 ± 3.1	23.7 ± 4.1	127.6 ± 36.0	2.3 ± 0.5
$Cr^{-/-}$	5	15.1 ± 4.7	22.7 ± 5.0	117.2 ± 28.5	2.2 ± 0.4

patch configuration is a consequence of long-term changes in the electrical membrane properties resulting from the mutation can be ruled out.

Our model should not be seen as a complex model of the granule cell, similar to the one proposed by D'Angelo et al. (2001), but rather as an abstract model focusing on a specific cell property, cytosolic Ca^{2+} buffering. The purpose of this model is to demonstrate the basic mechanism linking alteration of the intrinsic excitability in $Cr^{-/-}$ mice to alterations in the cytosolic Ca^{2+}-buffering capacity. Thus, on a broader perspective, the conclusions drawn from our simulations can be applied to other neuronal types, providing that the mechanisms of excitability are essentially the same as in cerebellar granule cells and that the conductance of the Ca^{2+}-activated K^+ channels is sufficient to obtain a strong coupling between excitability and Ca^{2+} dynamics during the spike generation. Although it is general knowledge that increasing Ca^{2+}-activated K^+ current slows down the firing rate, faster Ca^{2+} dynamics through reduced Ca^{2+} buffering has the opposite effect. The model suggests that this is because of direct control of $I_{K\text{-}Ca}$ by the Ca^{2+} transient, speeding up spike repolarization when the calcium-buffering capacity is decreased. Interestingly, experimental data obtained from hippocampal neurons perfused with BAPTA support our results (Lancaster and Nicoll, 1987; Storm, 1987). In this view, in addition to their obvious role in Ca^{2+} homeostasis, Ca^{2+}-binding proteins could play an active role in modulating neuronal intrinsic excitability and therefore neuronal plasticity. Although information storage is usually believed to be mediated by long-term modifications in the strength of synaptic transmission, activity-dependent changes in the neuronal intrinsic excitability also take place, causing forms of nonsynaptic plasticity. Such activity-dependent changes in intrinsic excitability have been shown to occur in cerebellar granule cells (Armano et al., 2000) and neurons of the deep cerebellar nuclei (Aizenman and Linden, 2000). It would be interesting to know whether activity-dependent modifications in the localization or in the level of expression of Ca^{2+}-binding proteins are involved. Although expression changes are still controversial (for review, see Baimbridge et al., 1992), changes in the localization of calretinin have been shown to occur in neurons (Hack et al., 2000).

Our results shed light on previous data obtained by Schiffmann et al. (1999), which show an increased simple-spike firing in Purkinje cells of alert $Cr^{-/-}$ mice. Because calretinin is not expressed in Purkinje cells, their firing alterations have to be an indirect consequence of the mutation. Indeed, because granule cells excite Purkinje cells through the parallel fibers, the increased Purkinje cell-firing rate observed *in vivo* can be explained by the increased granule cell excitability. Indeed, neither any increase in synaptic excitation was observed at the mossy fiber granule cell synapse nor excitatory transmission or short-term plasticity were altered at the parallel fiber Purkinje cell synapse in $Cr^{-/-}$ cerebellar slices (Schiffmann et al., 1999). Thus, altered intrinsic excitability in granule cells is probably the most important factor causing the *in vivo* alterations in $Cr^{-/-}$ mice.

The possibility that calretinin deficiency might increase excitability in other cerebellar neurons cannot be ruled out at present. Indeed, in rodents, calretinin is also present in two other neuronal subtypes of the granule cell layer: unipolar brush cells and Lugaro cells (Résibois and Rogers, 1992). Lugaro cells are believed to exert a disinhibitory influence on Purkinje cells via a glycinergic inhibition of Golgi cells (Dieudonné and Dumoulin, 2000). Therefore, an increased excitability of the Lugaro cells induced by the calretinin deficiency could lead to an increased activity at the level of the Purkinje cell. The involvement of unipolar brush cells may also cause a direct excitatory enhancement of Purkinje cells. However, it should be noted that unipolar brush cells are restricted to a subset of cerebellar lobes (Diño et al., 2000), whereas the increased Purkinje cell firing is ubiquitous in the cerebellar cortex of $Cr^{-/-}$ mice (G. Cheron, D. Gall, and S. N. Schiffman, personal communication).

In conclusion, this study demonstrates that calretinin deficiency increases the intrinsic excitability of cerebellar granule cells. The increased granule cell electroresponsiveness may explain the electrophysiological and behavioral alterations observed *in vivo* on alert $Cr^{-/-}$ mice, indicating the critical role of granule cells in information processing in the cerebellar cortex. On a broader perspective, we suggest that modulation of neuronal excitability by Ca^{2+}-binding proteins could play a functional role in the control of information coding and storage in the CNS.

References

Aizenman CD, Linden D (2000) Rapid, synaptically driven increase in the intrinsic excitability of cerebellar deep nuclear neurons. Nat Neurosci 3:109–111.

Armano S, Rossi P, Taglietti V, D'Angelo E (2000) Long-term potentiation of intrinsic excitability at the mossy fiber-granule cell synapse of rat cerebellum. J Neurosci 20:5208–5216.

Baimbridge KG, Celio M, Rogers J (1992) Calcium-binding proteins in the nervous system. Trends Neurosci 15:303–308.

Chay TR, Keizer J (1983) Minimal model for membrane oscillations in the pancreatic β-cell. Biophys J 42:181–190.

Cheung WY (1980) Calmodulin plays a pivotal role in cellular regulation. Science 207:19–27.

D'Angelo E, Rossi P, Taglietti V (1993) Different proportions of N-methyl-D-aspartate and non-N-methyl-D-aspartate receptor currents at the mossy fibre-granule cell synapse of developing rat cerebellum. Neuroscience 53:121–130.

D'Angelo E, Filippi GD, Rossi P, Taglietti V (1995) Synaptic excitation of individual rat cerebellar granule cells *in situ*: evidence for the role of NMDA receptors. J Physiol (Lond) 484:397–413.

D'Angelo E, Filippi GD, Rossi P, Taglietti V (1997) Synaptic activation of Ca^{2+} action potentials in immature rat cerebellar granule cells *in situ*. J Neurophysiol 78:1631–1642.

D'Angelo E, Filippi GD, Rossi P, Taglietti V (1998) Ionic mechanism of electroresponsiveness in cerebellar granule cells implicates the action of a persistent sodium current. J Neurophysiol 80:493–503.

D'Angelo E, Nieus T, Maffei A, Armano S, Rossi P, Taglietti V, Fontana A, Naldi G (2001) Theta-frequency bursting and resonance in cerebellar granule cells: experimental evidence and modeling of a slow K^+-dependent mechanism. J Neurosci 21:759–770.

Diño MR, Nunzi M, Anelli R, Mugnaini E (2000) Unipolar brush cells of the vestibulo-cerebellum: afferents and targets. In: Cerebellar modules, molecules, morphology and function (Gerrits N, Ruisgrok T, Zeeuw CJD, eds), pp 123–137. Amsterdam: Elsevier.

Dieudonné S, Dumoulin A (2000) Serotonin-driven long-range inhibitory connections in the cerebellar cortex. J Neurosci 20:1837–1848.

Edmonds B, Reyes R, Schwaller B, Roberts W (2000) Calretinin modifies presynaptic calcium signaling in frog saccular hair cells. Nat Neurosci 80:2521–2537.

Fierro L, Llano I (1996) High endogenous calcium buffering in Purkinje cells from rat cerebellar slices. J Physiol (Lond) 496:617–625.

Gabbiani F, Mitgaard J, Knoepfel T (1994) Synaptic integration in a model of cerebellar granule cells. J Neurophysiol 72:999–1009.

Galas M-C, Chasserot-Golaz S, Dirrig-Grosch W, Bader M (2000) Presence

of dynamin syntaxin complexes associated with secretory granules in adrenal chromaffin cells. J Neurochem 75:1511–1519.

Gall D, Susa I (1999) Effect of Na/Ca exchange on plateau fraction and $[Ca]_i$ in models for bursting in pancreatic β-cells. Biophys J 77:45–53.

Gall D, Gromada J, Susa I, Herchuelz A, Rorsman P, Bokvist K (1999) Significance of Na/Ca exchange for Ca^{2+}-buffering and electrical activity in mouse pancreatic β-cells. Biophys J 76:2018–2028.

Hack NJ, Wride M, Charters K, Kater S, Parks T (2000) Developmental changes in the subcellular localization of calretinin. J Neurosci 20:RC67.

Helmchen F, Imoto K, Sakmann B (1996) Ca^{2+} buffering and action potential-evoked Ca^{2+} signaling in dendrites of pyramidal neurons. Biophys J 70:1069–1081.

Hodgkin AL, Huxley A (1952) A quantitative description of membrane current and its application to conduction and excitation in nerve. J Physiol (Lond) 117:500–544.

Horn R, Marty A (1988) Muscarinic activation of ionic currents measured by a new whole-cell recording method. J Gen Physiol 92:145–159.

Ito M (1984) Granule cells. In: The cerebellum and neuronal control, pp 74–93. New York: Raven.

Lancaster B, Nicoll R (1987) Properties of two calcium activated hyperpolarizations in rat hippocampal neurones. J Physiol (Lond) 389:187–203.

Maex R, Schutter ED (1998) Synchronization of Golgi and granule cell firing in a detailed network of the cerebellar granule cell layer. J Neurophysiol 80:2521–2537.

Marini AM, Strauss K, Jacobowitz D (1997) Calretinin containing neurons in rat cerebellar granule cell cultures. Brain Res Bull 42:279–288.

Persechini A, Moncrief N, Kretsinger R (1989) The EF-hand family of calcium-modulated proteins. Trends Neurosci 12:462–467.

Peterson BZ, DeMaria C, Adelman J, Yue D (1999) Calmodulin is the Ca^{2+} sensor for Ca^{2+}-dependent inactivation of L-type calcium channels. Neuron 22:549–558.

Qin NR, Olcese R, Bransby M, Lin T, Birnbaumer L (1999) Ca^{2+}-induced inhibition of the cardiac Ca^{2+} channel depends on calmodulin. Proc Natl Acad Sci USA 96:2435–2438.

Résibois A, Rogers J (1992) Calretinin in rat brain: an immunohistological study. Neuroscience 46:101–134.

Roberts WM (1993) Spatial calcium buffering in frog saccular hair cells. Nature 363:74–76.

Schiffmann S, Cheron G, Lohof A, D'Alcantara P, Meyer M, Parmentier M, Schurmans S (1999) Impaired motor coordination and Purkinje cell excitability in mice lacking calretinin. Proc Natl Acad Sci USA 96:5257–5262.

Schurmans S, Schiffmann S, Gurden H, Lemaire M, Lipp H, Schwam V, Pochet R, Imperato A, Bohme G, Parmentier M (1997) Impaired long-term potentiation induction in dentate gyrus of calretinin-deficient mice. Proc Natl Acad Sci USA 94:10415–10420.

Silver RA, Traynelis S, Cull-Candy S (1992) Rapid time course of miniature and evoked excitatory currents at cerebellar synapses *in situ*. Nature 355:163–166.

Storm JF (1987) Intracellular injection of a Ca^{2+} chelator inhibits spike repolarization in hippocampal neurons. Brain Res 435:387–392.

Stuenkel EL (1994) Regulation of intracellular calcium and calcium buffering properties of rat isolated neurohypophysial nerve endings. J Physiol (Lond) 481:251–271.

Tatsumi H, Katayama Y (1993) Regulation of the intracellular free calcium concentration in acutely dissociated neurons from rat nucleus basalis. J Physiol (Lond) 464:165–181.

Traub RD, Llinas R (1979) Hippocampal pyramidal cells: significance of dendritic ionic conductances for neuronal functioning and epileptogenesis. J Neurophysiol 42:476–496.

Zuhlke RD, Pitt G, Deisseroth K, Tsien R, Reuter H (1999) Calmodulin supports both inactivation and facilitation of L-type calcium channels. Nature 399:159–162.